SMGroup

SM Journal of Bioinformatics and Proteomics

Research Article

Molecular Determinants for Recognition of Cell Surface Protein Receptor by Botulinum Neurotoxin B -A Quantum Chemical Analysis

Hui Yang[1,2] and Xiche Hu[2]*

[1]*Department of Biology, the Pennsylvania State University, University Park, USA*
[2]*Department of Chemistry and Biochemistry, University of Toledo, Toledo, USA*

Article Information

Received date: Mar 25, 2016
Accepted date: Jun 09, 2016
Published date: Jun 15, 2016

***Corresponding author**

Xiche Hu, Department of Chemistry and Biochemistry, University of Toledo, USA, Tel: (419)530-1513, Fax: (419)530-4033; Email: xhu@utoledo.edu

Keywords Bacterial toxin; Cell surface receptor; Protein-protein interaction; Molecular recognition; Quantum chemical calculation

Abbreviations BoNTs: Botulinum Neurotoxins; BoNT/B, BoNT Serotype B; Syt-II, Synaptotagmins (Syts) II; Hc, Carboxyl-domain of the heavy chain of BoNT/B; HcC, the C-terminal sub domain of the carboxyldomain of the heavy chain of BoNT/B; HcN, the N-terminal sub domain of the carboxyl-domain of the Heavy chain of BoNT/B

Abstract

Botulinum Neurotoxins (BoNTs) bind the neuronal membrane of the host cell via dual interactions with both protein receptors and gangliosides. In order to decipher the molecular determinants for recognition of cell surface protein receptor synaptotagmins II (Syt-II) by the BoNT serotype B (BoNT/B), a high-level quantum chemical analysis was performed, on the basis of the 2.15 *Å* resolution x-ray crystal structure of the BoNT/B – Syt-II complex. The work resulted in the discovery of two interfaces of molecular recognition; the amphipathic α–helix of the protein receptor Syt-II interacts with BoNT/B by forming a hydrophobic interface on one side of the helix and a hydrophilic interface on the other side. The hydrophobic interface consists of residues Phe47, Leu50, Phe54, Phe55 and Ile58 of Syt-II interacting with residues Trp1178, Tyr1181, Tyr1183, Phe1194 and Phe1204 of BoNT/B. The hydrophilic interface is composed of residues Lys53 and Glu57 of Syt-II interacting with residues Lys1113, Asp1115, Ser1116 and Lys1192 of BoNT/B. Intermolecular interaction energies between BoNT/B and Syt-II were calculated by means of the supermolecular approach at the MP2 level with subsequent solvation energy correction. It was found that the energetic contribution of the hydrophobic interface toward binding of BoNT/B with Syt-II (-9.49 kcal/mol) is much stronger than that of the hydrophilic interface (-2.58 kcal/mol). Furthermore, pair-wise intermolecular interaction analysis led to the findings that π-π stacking interactions among aromatic residues are the major molecular determinants for recognition of cell surface protein receptor Syt-II by the botulinum neurotoxin BoNT/B. These findings are significant since it was widely believed that the extreme toxicities of BoNTs have a lot to do with the high affinity and specificity of their binding to the neuronal membrane. It is expected that a detailed understanding of the intermolecular interactions responsible for the extreme specificity of molecular recognition between BoNT and its protein receptor as reported here will have far reaching implication for not only the rational design of potent protein toxin inhibitors targeting toxin-protein receptor binding interface but also the development of more suitable therapeutic neurotoxins.

Introduction

Botulinum neurotoxins (BoNTs[1]) are potent protein toxins produced by the bacterium *Clostridium botulinum*. They are among the most poisonous toxins known to mankind, with a Lethal Dose (LD_{50}) value below 1 ng/kg [1]. There exist seven serologically distinct BoNTs, commonly known as serotype A-G [2,3] that are classified on the basis of the lack of antitoxin cross-neutralization. Although experimental evidence indicates that humans are sensitive to all serotypes, natural intoxications occur only with BoNT/A, BoNT/B, BoNT/E and BoNT/F [4-6]. BoNT exerts its action on its host as a zinc metalloprotease by targeting SNARE (soluble N-ethylmaleimide-sensitive factor attachment protein receptor) proteins. The cleavage of SNARE proteins blocks the release of the neurotransmitter acetylcholine at the nerve ending, resulting in flaccid paralysis. As a protein toxin, BoNT intoxicates cell via a typical four-step process composed of binding, internalization, membrane translation and enzymatic target modification [7,8].

Decades of biochemical investigations have led to the realization that the extreme toxicities of BoNTs have a lot to do with the high affinity and specificity of their binding to the neuronal membrane [9-11]. It is now commonly accepted that binding of BoNTs occurs via a "dual-receptor" model as originally proposed by Montecucco and coworkers [12]: complex gangliosides act as a low affinity acceptor responsible for accumulating the toxins on the neuronal membrane, facilitating a subsequent binding of BoNTs to a second protein receptor. In spite of the fact that the seven BoNT serotypes A-G [2,3] share certain structural and functional similarity, different protein receptors are utilized by the seven BoNT serotypes as the co-receptor. A major focus of the field over the years was to identify the receptor and pathway for each BoNT. Two homologous synaptic vesicle proteins, synaptotagmins (Syts) I and II [13,14] were identified to be the protein receptor for BoNT/B and BoNT/G [15-18], whereas the 12 transmembrane domain synaptic vesicle protein 2 (SV2) [19,20] mediates the entry of BoNT/A, BoNT/E and BoNT/F [9,21-24]. In the case of BoNT/B, it was found that the molecular recognition domain only consists of residue 40-60 located in the luminal domain of Syt-II [18].

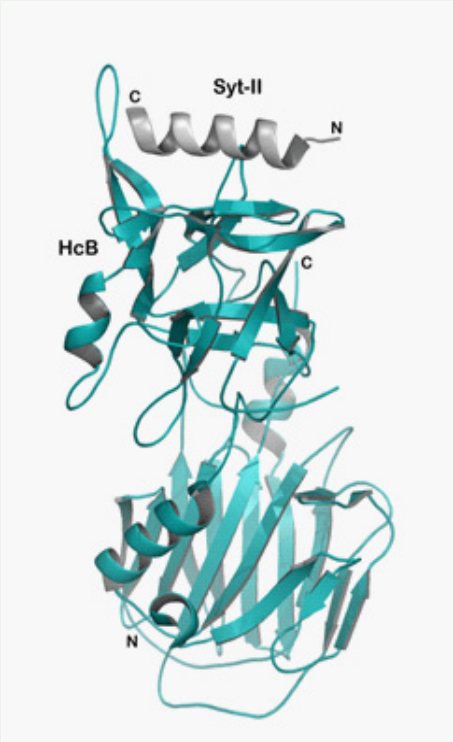

Figure 1: **(a)** Structure of the complex between the carboxyl-domain of the heavy chain (Hc) of BoNT/B (colored in cyan) and synaptotagmin II (Syt-II) (colored in gray) based on the 2.15 *Å* resolution x-ray crystal structure of the complex (PDB ID: 2NM1) [32]. The Hc domain consists of an amino terminal lectin-like jelly roll subdomain (HcN) and a carboxyl-terminal *β*-trefoil subdomain (HcC). (This plot is generated with the program PyMOL [34]).

The structural organization of BoNT is functionally related to its mechanism of action. The known crystal structures of BoNT serotypes, BoNT/A, BoNT/B and BoNT/G [25-27], revealed that all BoNTs adopt similar fold, composing of multiple functionally independent domains that perform the associated tasks in the four-step mechanism of intoxication. Each BoNT is initially synthesized as a single chain precursor protein of ~150 kDa mass that is cleaved by bacterial or host proteases into two chains: a light chain (L) of ~50 kDa and a heavy chain (H) of ~100 kDa. The former functions as a metalloprotease; and the latter contains an amino-terminal domain (H_N) that facilitates the translocation of the light chain from endosomes into the cytosol, and a carboxyl-terminal domain (H_C) that mediates the binding to specific cell surface receptors. Furthermore, numerous evidence indicates that it is the C-terminal subdomain of the carboxyl-domain of the heavy chain of BoNT (HcC) that binds directly with the cell surface receptors [2,17,18,28,29]. Interestingly, HcC retains a full binding affinity as an isolated fragment [30].

Our knowledge of binding, as the critical event in the four-step processes, was further advanced by the determination of co-crystal structures of BoNT/B with the receptors. In 2006, the x-ray crystal structure for the full length BoNT/B in complex with the Syt-II recognition domain was determined to 2.6 *Å* resolutions [31]. At the same time, a 2.15 *Å* resolution x-ray crystal structure was reported for a recombinant fusion protein consisting of the Hc-fragment of BoNT/B and the luminal domain of Syt-II [32]. Recently, the crystal structure of the ternary complex of BoNT/B with both its protein receptor Syt-II and its gangliosides receptor GD1a was determined to 2.3 *Å* resolutions [33]. The very existence of the crystal structure of the ternary complex provided direct proof of the dual receptor model [12] at the structural level. Furthermore, it was demonstrated that the protein receptor Syt-II and the gangliosides receptor GD1a occupy separate binding sites with no allosteric effect, i.e., the binding affinity of BoNT/B towards Syt-II was not influenced by the presence of GD1a [33].

Our main objective here is to understand the molecular determinants for molecular recognition of the protein receptor by botulinum neurotoxin. The co-crystal structures [31-33] reveal structural insight into the toxin-protein receptor interactions, which form the basis of the quantum mechanical analysis presented here. Interestingly, it was discovered that the luminal domain of Syt-II undergoes a structural transition from totally unstructured into an *α*-helix upon binding with BoNT/B [31,32]. As shown in Figure 1(a,b), the induced *α*-helix consisting of residues 47-58 of Syt-II binds to the distal tip of HcC of BoNT/B, in a saddle-shaped crevice on the surface formed by eight *β*-sheets and four intervening loops.

In this article, a high-level quantum chemical analysis is performed, on the basis of the 2.15 *Å* resolution x-ray crystal structure of the BoNT/B – Syt-II complex [32], to determine the molecular determinants for recognition of the protein cell surface receptor by botulinum neurotoxin. The work resulted in the discovery of multiple modes of molecular recognition in the formation of the BoNT/B – Syt-II complex. It is expected that a detailed understanding of the intermolecular interactions responsible for the extreme specificity of molecular recognition between BoNT and its protein receptor as reported here will have far reaching implication for not only the rational design of potent protein toxin inhibitors targeting the toxin-protein receptor binding interface but also the development of more suitable therapeutic neurotoxins [6,11,35].

Theory and Methods

The conceptual framework for the protein-protein complex formation in solution is depicted in the following scheme,

$$\begin{array}{ccc} A(aq) + B(aq) & \xrightarrow{\Delta G^{aq}_{complex}} & AB(aq) \\ \Delta G^{sol}_{A}\uparrow \quad \Delta G^{sol}_{B}\uparrow & & \Delta G^{sol}_{AB}\uparrow \\ A(g) + B(g) & \xrightarrow[\Delta G^{g}_{Int}]{} & AB(g) \end{array} \qquad (1)$$

(b)

```
Human   MRNIFKRNQEPIVAPATTTATMPIG---PVDNSTESGGAGESQEDMFAKLKEKLFNEINK 57
Mouse   MRNIFKRNQEPNVAPATTTATMPLAPVAPADNSTESTGPGESQEDMFAKLKEKFFNEINK 60
        ********** **********:.   *_****** *_**************:******
```

Figure 1: (b) The sequence of the intraluminal domain of the human Synaptotagmin II and its alignment with that of the mouse.

Citation: Yang H and Hu X. Molecular Determinants for Recognition of Cell Surface Protein Receptor by Botulinum Neurotoxin B-A Quantum Chemical Analysis. SM J Bioinform Proteomics. 2016; 1(1): 1005.

This serves as a basis for our analysis of the binding affinity of BoNT/B to Syt-II. It is worth noting that a similar scheme was used to calculate solution phase binding affinities for ligand-protein complexes previously [36]. Both proteins (BoNT/B and Syt-II) are solvated before complex formation. They both lose part of their solvation shell upon binding, which incurs an energy cost commonly referred to as dehydration energy. According to the scheme, the binding energy for complex formation in solution can be evaluated indirectly by calculating intermolecular interaction energies in the gas phase (ΔE^{g}_{int}) followed by a correction for the dehydration energy (ΔE_{Deh}):

$$\triangle E^{aq}_{complex} = \triangle E_{\text{int}} + \triangle E_{Deh} \qquad (2)$$

The gas phase intermolecular interaction energies between Syt-II and its surrounding residues in BoNT/B (ΔE^{g}_{int}), were calculated by means of the supermolecular approach. In the supermolecular approach, the energy of interaction between molecules A and B is defined as the difference between the energy of the interacting dimer E_{AB} and the energies of the monomers E_A and E_B

$$\Delta E = E_{AB} - E_A - E_B$$

The calculations were carried out at the second order Moller-Plesset Theory (MP2) level with a frozen core using the GAUSSIAN 03 program [37] on HP Z800 workstations installed in our lab and the Oakley Cluster of Intel Xeon CPUs at the Ohio Supercomputer Center. The Basis Set Superposition Error (BSSE) was corrected by the Boys and Bernardi Counter Poise Method [38].

As in all other quantum mechanical calculations, the quality of calculated results depends on the proper choice of the basis set. Non-bonded intermolecular interaction is essentially a juxtaposition of several elements, including the electrostatic interaction, the exchange repulsion interaction, induction, and the dispersion force. For hydrogen bond and salt-bridge, electrostatic interaction is the dominant force. The standard 6-31+G* method has been widely used to treat hydrogen bonded complexes of large biomolecular systems like ours since more sophisticated treatment is prohibited by the size of the investigated system [39,40]. We will adopt the MP2/6-31+G* method for treating all salt-bridge and hydrogen bonding interactions. The dispersion force is the dominant attractive force between neutral molecules [41-43], which occurs in both π-π stacking and CH-π interaction. The dispersion force arises from the mutual correlation of electrons that belong to interacting monomers (intermolecular correlation effects). The correlation energy is typically of the same order of magnitude as the intermolecular interaction energy. Consequently, the inclusion of electron correlation is important in any accurate *ab initio* electronic structure calculation of weakly bonded complexes. It has been shown that for a proper treatment of π-π stacking and CH-π interaction, the inclusion of diffuse basis sets is required [39,44]. These diffuse basis sets are localized sufficiently far from the atomic nuclei, and thus fill the empty space between two interacting monomers. The latter is where a substantial portion of correlation energy originates. At the MP2 level, Dunning's correlation consistent basis sets (cc-pVXZ, X=D, T, Q, and 5) and the augmented aug-cc-PVXZ basis sets are desirable, and have been applied to both π-π stacking and hydrogen-bonding complexes of small molecules [45,46].

However, such huge basis sets are not computationally feasible for the large system of our interest here. A more feasible choice for our system is a medium sized basis set, such as the polarization augmented double zeta 6-31G* basis set. In a series of studies of DNA base stacking, Hobza and co-workers employed a modified 6-31G* basis set with diffuse (momentum optimized, dispersion energy-optimized) d-polarization at the MP2 level of theory [39,47]. In the conventional 6-31G* basis set, the d-polarization functions for non-hydrogen atoms (C, N, and O atoms) are energy-optimized with an exponent of 0.8. In the modified basis set, an exponent of 0.25 is used for the d-polarization functions of C, N, and O atoms, instead. Following the author's convention [47,48], the modified basis set is designated 6-31G*(0.25). The 6-31G*(0.25) basis set will be used in all of our calculations of π-π stacking and CH-π interactions. Accordingly, the chosen MP2 method with 6-31G*(0.25) basis set will be denoted MP2/6-31G*(0.25) method.

The dehydration energy for the complex formation is defined (see Eq. 1) by

$$\Delta E_{Deh} = \Delta G^{sol}_{AB} - \Delta G^{sol}_{A} - \Delta G^{sol}_{B} \qquad (3)$$

where ΔG^{sol}_{i}, i = AB, A, B represents the free energies of solvation for the complex AB, and the monomers A, B, respectively. Due to the prohibitively high cost of explicitly including solvent molecules in simulating biological systems, a common way to calculate the free energy of solvation is through continuum models. Here, we adopted the SM5.42R Solvation Model of Cramer and Truhlar [49] as implemented in the GAMESOL-v3.1 package [50] and the 2008 R1 version of GAMESS [51] for evaluation of the free energy of solvation. In the SM5.42R model, the standard-state free energy of solvation includes two components: the electrostatic term and the first solvation shell term (or nonelectrostatic term). As the solute is solvated, the charge distribution of the solute induces a polarization of the surrounding dielectric medium of the solvent, and the electric polarization field of the solvent, in turn, interacts with the solute charge distribution in a self-consistent manner. The electrostatic term consists of the electrostatic free energy of electric polarization of the solvent (including the solvent reorganization cost) and the distortion cost of polarizing the solute to be self-consistent with the solvent electric polarization. Theoretically, the mutual polarization of solute and solvent is implicitly accounted for by self-consistently solving the Schrödinger equation that contains an extra solvent reaction field operator (V_R) in the presence of solute:

$$(H^{0} + \frac{1}{2}V_R)\psi = E\psi \qquad (4)$$

where H^{0} is the gas phase Hamiltonian. Mathematically, the electrostatic component of the free energy of solvation is obtained by taking the difference between the energy (i.e., eigenvalue E) of eq. (4) and that associated with the gas phase Schrödinger equation. The nonelectrostatic term includes contributions arising from cavity creation, dispersion, and free energy changes derived from local perturbations in solvent structure.

Depending on the gas phase Hamiltonian (H^{0}), the SM5.42R model has been parameterized at various levels of theory, such as SM5.42R/HF-6-31+G*, SM5.42R/PM3 (Parameterized Model 3), and etc [49]. The accuracy of the SM5 model has been extensively calibrated [49]. Mean unsigned errors between calculated and experimental free energies of solvation are typically 0.4-0.5 kcal/mol for neutral solutes. For ionic solutes in water, the mean unsigned

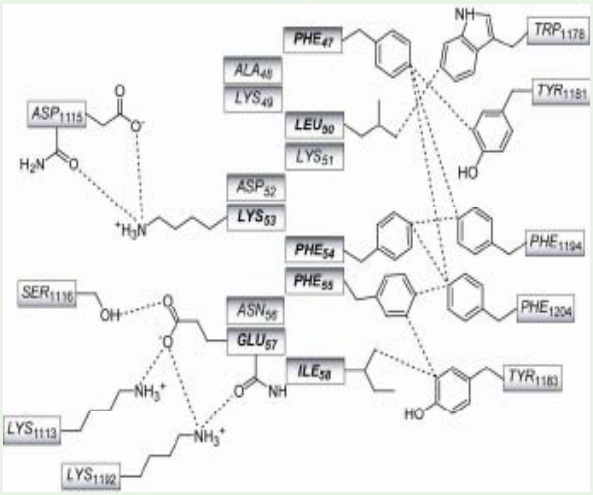

Figure 2: Intermolecular interaction map between the synaptotagmin II (Syt-II) helix (center) and the C-terminal subdomain of the carboxyl-domain of the heavy chain (HcC) of BoNT/B [32]. The Hydrophobic interface (right) consists of residues F47, L50, F54, F55 and I58 of Syt-II and residues W1178, Y1181, Y1183, F1194 and F1204 of HcC from BoNT/B. The hydrophilic interface (left) is composed of residues K53 and E57 of Syt-II and residues K1113, D1115, S1116 and K1192 of HcC from BoNT/B. Dash lines indicate the closest interacting atoms of the interacting partners between Syt-II and HcC of BoNT/B.

error is 3.5-3.9 kcal/mol for the SM5.42R/HF model [49]. In our calculations, the SM5.42R Solvation Model was applied at the HF/6-31+G* level. SCF scheme *II* as defined in [49] was used to achieve better convergence and the dielectric constant of water solvent was set to 78.

Table I: Intermolecular interaction energies in the hydrophobic interface.

Intermolecular pairs				
Syt-II	HcC of BoNT/B	ΔE^{g}_{HF} (kcal/mol)[a]	ΔE^{g}_{MP2} (kcal/mol)[a]	ΔE^{s} (kcal/mol)[b]
Phe47 Phe54 Phe55 Leu50 Ile58	Tyr1181 Tyr1183 Phe1194 Phe1204 Trp1178	12.01	-13.99	-9.49
CH – π interaction				
Ile58	Tyr1183	0.08	-0.51	-0.43
Leu50	Trp1178	1.57	-0.27	-0.10
π – π stacking interaction				
Phe47	Tyr1181 Phe1194 Phe1204	1.29	-3.29	-2.40
Phe54	Tyr1183 Phe1194 Phe1204	5.84	-5.46	-4.50
Phe55	Tyr1183 Phe1204	2.95	-2.73	-2.11

a. Gas-phase intermolecular interaction energies (in kcal/mol) at the MP2/6-31G*(0.25) level (ΔE^{g}_{MP2}) and HF/6-31G*(0.25) level (ΔE^{g}_{HF}) are corrected for BSSE.

b. Solution phase interaction energies (in kcal/mol) are estimated by applying the SM5.42R model of Cramer and Truhlar at the HF/6-31+G* level.

Results

A careful examination of the crystal structure of the BoN4T/B – Syt-II complex in three-dimensional computer visualization resulted in the discovery of multiple modes of molecular recognition in the formation of the BoNT/B – Syt-II complex. It was found that the α-helix consisting of residues 47-58 of Syt-II (see Figure 1(b)) is largely amphipathic where one surface of the alpha helix is mainly lined up with hydrophilic residues Lys49, Asp52, Lys53, Asn56, Glu57 and the opposite face is dominated by hydrophobic residues Phe47, Leu50, Phe54, Phe55, and Ile58. Figure 2 shows the amphipathic α-helix of Syt-II, along with its interacting residues in the C-terminal subdomain of the carboxyl-domain of the heavy chain (HcC) of BoNT/B. As can be seen, hydrophilic residues of Syt-II interact with hydrophilic residues of BoNT/B, whereas hydrophobic residues of Syt-II interact with hydrophobic residues of BoNT/B, forming two interfaces of binding interactions for molecular recognition. The hydrophobic interface (right) consists of residues Phe47, Leu50, Phe54, Phe55 and Ile58 of Syt-II interacting with residues Trp1178, Tyr1181, Tyr1183, Phe1194 and Phe1204 of HcC of BoNT/B. The hydrophilic interface (left) is composed of residues Lys53 and Glu57 of Syt-II interacting with residues Lys1113, Asp1115, Ser1116 and Lys1192 of HcC of BoNT/B. Detailed three-dimensional arrangements of both interfaces are depicted in a stereo pair drawing in Figure 3.

Intermolecular interaction energies between BoNT/B and its receptor protein Syt-II were calculated by means of the supermolecular approach at the MP2 level based on the 2.15 *Å* resolution x-ray crystal structure of the BoNT/B – Syt-II complex (see Figure 1(a)). Two sets of calculations were carried out, i.e., (i) interactions in the hydrophobic interface and the hydrophilic interface between Syt-II and BoNT/B, respectively; and (ii) pairwise interactions between Syt-II and several major structural motifs of BoNT/B. Given the large system size of our study, it is not computationally feasible to use a very large basis set at the level of theory of our choice (i.e., MP2). Past experience of ours and others demonstrated that a proper medium sized basis set can be chosen according to the physical nature of the intermolecular interaction [52-54]. As described in the Method section, the standard MP2/6-31+G* method was used to treat all salt-bridge and hydrogen bonding interactions whereas the MP2/6-31G*(0.25) method was utilized to deal with π-π stacking and CH-π interactions. The coordinates of non-hydrogen atoms in Syt-II and their interacting residues in BoNT/B were extracted from the 2.15 *Å* resolution x-ray crystal structure of the BoNT/B – Syt-II complex (PDB accession number 2NM1) [32]. Therefore, the internal coordinates of the monomers used in computing E^{g}_{A} and E^{g}_{B} was the same as within the dimer AB in the supermolecular approach. The positions of all hydrogen atoms were placed by *ab initio* geometry optimization at the HF/6-31G* level with all the non-hydrogen atom positions fixed.

The first set of calculations aims at quantifying and comparing the binding strength of the hydrophobic interface against that of the hydrophilic interface of the BoNT/B – Syt-II complex. For the hydrophobic interface, side chains of residues Phe47, Leu50, Phe54, Phe55, Ile58 of Syt-II bind with side chains of residues Trp1178, Tyr1181, Tyr1183, Phe1194, Phe1204 of BoNT/B through multiple π-π stacking and CH-π interactions. The strength of the overall interaction energy for the entire hydrophobic interface was calculated at the MP2/6-31G*(0.25) level of theory. The results of

Table II: Intermolecular interaction energies in the hydrophilic interface.

Intermolecular pairs				
Syt-II	HcC of BoNT/B	ΔE^{g}_{HF} (kcal/mol)[a]	ΔE^{g}_{MP2} (kcal/mol)[a]	ΔE^{s} (kcal/mol)[b]
Glu57 Lys53 O57	Lys1113 Lys1192 Ser1116 Asp1115 O_{1115}	-215.07	-220.52	-2.58
Salt bridge				
Glu57	Lys1113	-119.54	-120.25	-1.08
Glu57	Lys1192	-107.74	-110.44	-1.07
Lys53	Asp1115	-55.91	-57.66	-0.27
Hydrogen bond				
O57 (Glu57 main chain)	Lys1192	-14.54	-14.06	-1.10
Glu57	Ser1116	-13.58	-14.63	-1.89
Lys53	O_{1115} (Asp1115 main chain)	-19.33	-20.41	0.31

a. Gas-phase intermolecular interaction energies (in kcal/mol) at the MP2/6-31+G* level (ΔE^{g}_{MP2}) and HF/6-31+G* level (ΔE^{g}_{HF}) are corrected for BSSE.
b. Solution phase interaction energies (in kcal/mol) are estimated by applying the SM5.42R model of Cramer and Truhlar at the HF/6-31+G* level.

the calculation are listed in Table I, with a total interaction energy of -13.99 kcal/mol at the MP2/6-31G*(0.25) level in the gas phase. Taking into consideration of the dehydration energy (4.5 kcal/mol), we obtained a solution phase interaction energy of -9.49 kcal/mol for the hydrophobic interface. For the hydrophilic interface, side chains of Lys53, Glu57 and the main chain carboxyl group of Glu57 of Syt-II interact with side chains of Lys1113, Asp1115, Ser1116, Lys1192, and the main chain carboxyl group of Asp1115 of BoNT/B through several salt-bridge and hydrogen bonding interactions. The strength of the overall interaction energy for the entire hydrophilic interface was calculated at the MP2/6-31+G* level, resulting in a total interaction energy of –220.52 kcal/mol in the gas phase (as shown in Table II). As expected, the gas phase interaction energy of –220.52 kcal/mol for the hydrophilic interface is much stronger than that of the hydrophobic interface (-13.99 kcal/mol). However, the energetic cost of desolvation for the hydrophilic interface is much higher (217.94 kcal/mol) since the constituting residues are either charged or polar, and well solvated in the monomeric state before the formation of the BoNT/B – Syt-II complex. As a result, the net interaction energy for the entire hydrophilic interface is only -2.58 kcal/mol at the MP2/6-31+G* level after taking into account of the desolvation energy. Overall, the results of our calculations showed that the energetic contribution from the hydrophobic interface toward binding of BoNT/B with Syt-II is much larger than that from the hydrophilic interface. The above finding of the dominant role played by the hydrophobic interface is in good agreement with results of a biophysical experiment reported in the literature [32]. In [32], isothermal titration calorimetry experiment was conducted to investigate the thermodynamics of the Syt-II – BoNT/B complex formation. Based on the observed large negative heat capacity change ($\triangle C_p$) upon complex formation, Jin *et al* concluded that the protein-protein interaction in the Syt-II – BoNT/B complex was driven by the hydrophobic effect.

The second set of calculations is essentially an interaction energy partitioning analysis, aiming at deciphering the molecular determinants for recognition of BoNT/B by Syt-II. The interest lies in determining which types of interactions are utilized by the protein receptor Syt-II for recognition of BoNT/B, and what their relative importance is. As shown in Figures 2 and 3 and listed in Tables I and II, the constituting interactions in the hydrophobic interface are mainly CH – π interactions (between Ile58 of Syt-II and Tyr1183 of BoNT/B; between Leu50 of Syt-II and Trp1178 of BoNT/B) and π -π stacking interactions among aromatic residues (Phe47 of Syt-II with residues Tyr1181, Phe1194, Phe1204 of BoNT/B; Phe54 of Syt-II with residues Tyr1183, Phe1194, Phe1204 of BoNT/B; Phe55 of Syt-II with residues Tyr1183, Phe1204 of BoNT/B). The constituting interactions for the hydrophilic interface are salt bridges (Glu57 of Syt-II with Lys1113 of BoNT/B; Glu57 of Syt-II with Lys1192 of BONT/B; Lys53 of Syt-II with Asp1115 of BoNT/B) and hydrogen bonds (main chain carboxyl oxygen of Glu57 of Syt-II with Lys1192 of BoNT/B; Glu57 of Syt-II with Ser1116 of BoNT/B; Lys53 of Syt-II with the main chain carboxyl oxygen of Asp1115 of BoNT/B). Pair wise interaction energies were calculated at the MP2 level of theory, and listed in Tables I and II under the separate headings of *π-π stacking interaction, CH-π interactions, salt bridge, and Hydrogen Bonding*.

As can be seen from Tables I and II, *π-π stacking interactions* dominate the binding interactions between BoNT/B and its protein receptor Syt-II. CH-π interactions also contribute to binding; albeit by a much smaller magnitude (see Table I). Among the *π-π stacking interactions* motifs, the binding interaction between Phe54 of Syt-II and aromatic residues Tyr1183, Phe1194, Phe1204 of BoNT/B is the strongest, with gas phase and solution phase interaction energy of -5.46 kcal/mol and -4.50 kcal/mol, respectively. Significant binding strengths are also contributed by π-π stacking interactions between Phe47 of Syt-II and aromatic residues Tyr1181, Phe1194, Phe1204 of BoNT/B, and those between Phe55 of Syt-II and aromatic residues Tyr1183, Phe1204 of BoNT/B, with a solution phase interaction energy of -2.40 kcal/mol and -2.11 kcal/mol (see Table I), respectively.

In contrast, hydrogen bandings and salt bridges make a smaller, but still significant contribution to binding. The salt bridges between Glu57 of Syt-II and Lys1113 of BoNT/B has a large gas phase MP2/6-31+G* interaction energy of -120.25 kcal/mol. However, when dehydration energy is taken into consideration, solution phase interaction energy of only -1.08 kcal/mol remains. Similarly, the interaction energies at the MP2 level for salt bridges between Glu57 of Syt-II and Lys1192 of BoNT/B and between Lys53 of Syt-II and Asp1115 of BoNT/B are -1.07 kcal/mol and -0.27 kcal/mol after solvation energy correction, respectively. The contribution of hydrogen bonding toward the formation of the Syt-II – BoNT/B complex ranges from -1.10 kcal/mol for the hydrogen bond between the main chain carboxyl oxygen of Glu57 of Syt-II and Lys1192 of BoNT/B, to -1.89 kcal/mol for the hydrogen bond between Glu57 of Syt-II and Ser1116 of BoNT/B. There is essentially no contribution to binding from the hydrogen bond between Lys53 of Syt-II and the main chain carboxyl oxygen of Asp1115 of BoNT/B.

Discussion

Since different basis sets were chosen to calculate interaction energies for different types of nonbonded interactions, i.e., 6-31+G* for all salt-bridge and hydrogen bonding interactions, and 6-31G*(0.25)

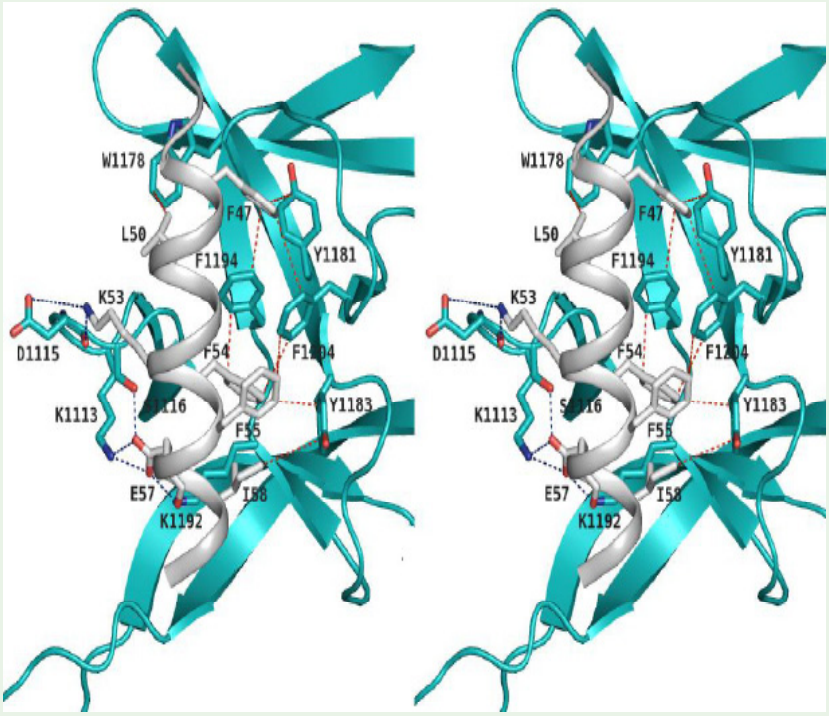

Figure 3: Stereo drawing of the synaptotagmin II (Syt-II) helix (colored in gray) binding interfaces with the C-terminal subdomain of the carboxyl-domain of the heavy chain (HcC) of BoNT/B (colored in cyan) based on the 2.15 *Å* resolution x-ray crystal structure of the complex of BoNT/B with Syt-II (PDB ID: 2NM1) [32]. The hydrophobic interface consists of residues F47, L50, F54, F55 and I58 of Syt-II and residues W1178, Y1181, Y1183, F1194 and F1204 of HcC from BoNT/B. The hydrophilic interface is composed of residues K53 and E57 of Syt-II and residues K1113, D1115, S1116 and K1192 of HcC of BoNT/B. Dash lines indicate the closest interacting pairs between Syt-II and HcC of BoNT/B. [This plot is generated with the program PyMOL (34)].

for π-π stacking and CH-π interactions, one important issue to address is the basis set dependence of our results. Although the large system size of the entire interface limited our adoption of a large basis set, it was computationally feasible to employ the 6-311++G** basis set for the decomposition analysis calculation (i.e., the second set of calculations above). For comparison, two representative pairs for the respective types of intermolecular interactions were analyzed for basis set dependence: the hydrogen bond between Glu57 of Syt-II and Ser1116 of BoNT/B, and π-π stacking interactions between Phe47 of Syt-II and aromatic residues Tyr1181, Phe1194, Phe1204 of BoNT/B. The MP2/6-311++G** calculations yielded a gas phase interaction energy ( ) of -14.74 kcal/mol for the former and -3.51 kcal/mol for the latter. Those are nearly the same as the corresponding results obtained by the MP2/6-31+G* calculation (-14.63kcal/mol) for the hydrogen bond and the MP2/6-31G*(0.25) calculation for π-π stacking interactions (-3.29 kcal/mol) as listed in Tables I and II. This comparative analysis of basis set dependence indicates that our choice of 6-31+G* for calculation of salt-bridge and hydrogen bonding interactions, and the 6-31G*(0.25) for π-π stacking and CH-π interactions are adequate. That is not unexpected since our choice of basis set was based on the physical nature of intermolecular interactions.

The results of our calculations presented above clearly point out π-π stacking interactions among aromatic residues as the major molecular determinants for recognition of cell surface receptor Syt-*II* by the botulinum neurotoxin BoNT/B. This finding is in good agreement with results of site-directed mutagenesis experiments [31,32,55-58]. In [32], Jin *et al* performed a site-directed mutagenesis analysis at or around the toxin-receptor interface between BoNT/B and the luminal domain of Syt-II. On the BoNT/B side, when the aromatic residues F1194 and F1204 were mutated to Ala, pull-down assay using GST–Syt-II wild type as bait showed drastically reduced binding. And this reduction of binding was correlated with marked reduction of toxicity [32]. On the Syt-II side, it was found that single point mutations of aromatic residues F47A, F54A, F55A abolished binding with BoNT/B [32]. Similar past and recent site-directed mutagenesis experiments re-affirmed the important role played by aromatic residues F47, F54 and F55 of Syt-II in binding with BoNT/B, as well as the highly homologous BoNT/G [31,56-58]. In particular, the latest pull-down assays [55,57] clearly showed that F54A mutant of Syt-II had the strongest diminishing effect on binding among the three mutants. Figure 6A of [55] revealed that the F54A mutant of the protein receptor Syt-II abolished binding with BoNT/B completely with and without gangliosides, whereas the binding with BoNT/B could be partially recovered to a very small extent by the addition of gangliosides for the F47A and F55A mutants. Figure 3 of [57] shown directly a 92% (estimated based on the bar chart) reduction of binding for the F47A mutant *vs* a near 100% reduction of binding for the F54A and F55A mutants. The fact that aromatic residues on both sides of the hydrophobic interface of BoNT/B and Syt-II were crucial for achieving toxin binding with the protein receptor provides strong support for our findings that aromatic π-π stacking interactions are the molecular determinants for binding.

Moreover, the impact of this research will go far beyond an

understanding of molecular recognition of BoNT/B by Syt-II. As stated earlier, botulinum neurotoxins are among the most poisonous toxins known to mankind. Molecular recognition of the neurotoxin by its cell surface receptor is at the center of its biological function, and a profound understanding of the underlying non-bonded interactions is required to intervene in a rational way to block the action of neurotoxin. On the basis of the aforementioned correlation (see above paragraph) between the reduction of binding of mutated BoNT/B (F1194A and F1204A) with its protein receptor Syt-II and the decreased toxicity of the mutated BoNT/B [32], our findings of π-π stacking interactions as the molecular determinants for recognition of cell surface receptor Syt-II by BoNT/B has direct implication for molecular design of therapeutics.

As shown in [Figures 2 and 3] both aromatic residues Phe1194 and Phe1204 of BoNT/B are in close geometric proximity of Phe47 and Phe54 of Syt-II for strong π-π stacking interactions. In addition, Phe1204 of BoNT/B is also in contact with Phe54 of Syt-II. Targeting the toxin-protein receptor binding interface, one can design competitive inhibitors that block binding of BoNT/B with the protein receptor to inhibit the toxic action of BoNT/B. Since π-π stacking interactions dominate the interface binding, a natural choice for effective inhibitors is aromatic molecules situated at same positions of F47, F54, F55 as in the bound complex [31,32]. Given the urgent need to combat potential bioterrorism with botulinum neurotoxins [4,59], it is hoped that this work will stimulate the bioscience community to take immediate action to experiment with such inhibitors.

As a matter of fact, there existed already strong evidence that had proven indirectly the validity of the proposed inhibitor design strategy. It has been observed that rimabotulinumtoxinB had an approximately 10-fold lower potency for the treatment of cervical dystonia in human versus mouse [see [56] and references therein]. Stormier *et al* analyzed this species difference at the molecular level, and attributed the receptor recognition as the possible origin of the observed potency difference. It turned out that human Syt-II is not a high affinity receptor for BoNT/B in comparison with mouse Syt-II [55,56]. Depicted in [Figure 1(b).] is the sequence alignment between human and mouse for the intraluminal domain of Syt-II, of which residues 47-60 were known to be associated with toxin-binding [31]. As can be seen, the only difference between human and mouse Syt-II within the toxin-binding site is that Leu51 of human Syt-II occurs in a corresponding position of Phe54 in mouse Syt-II. Accordingly, a mouse Syt-II 1–61 F54L mutant that mimics human Syt-II was created, and its ability to bind BoNT/B was tested in pull down assays. It was found that the Syt-II F54L mutant had diminishing binding with BoNT/B, which led to the conclusion that the human Syt-II with Leu51 in a corresponding position had a weak binding affinity with BoNT/B. It was then argued that drastically impaired receptor recognition by BoNT/B was responsible for its decreased potency in humans [56]. In light of this argument, it is worth noting that our quantum mechanical calculation identified Phe54 of Syt-II as the strongest contributor to binding of BoNT/B with Syt-II (see above). It is, thus, reasonable to expect that inhibitors consisting of aromatic moieties that preferentially target the site occupied by Phe54 of Syt-II should hold the greatest promise. For the same reason, sites occupied by Phe47 and Phe55 of Syt-II should also be targeted due to their substantial strength of interactions with the aromatic residues of BoNT/B as calculated in this work (see Table II). Better yet, a single inhibitor conjoined by aromatic moieties targeting all three sites should also be attempted.

Conclusion

The work resulted in the discovery of multiple modes of molecular recognition in the formation of the BoNT/B–Syt-II complex. The amphipathic α-helix of the protein receptor Syt-II interacts with the neurotoxin BoNT/B by forming two interfaces of binding interactions, a hydrophobic interface and a hydrophilic interface, for molecular recognition. The hydrophobic interface consists of residues Phe47, Leu50, Phe54, Phe55 and Ile58 of Syt-II interacting with residues Trp1178, Tyr1181, Tyr1183, Phe1194 and Phe1204 of BoNT/B. The hydrophilic interface is composed of residues Lys53 and Glu57 of Syt-II interacting with residues Lys1113, Asp1115, Ser1116 and Lys1192 of BoNT/B. The binding strength of the hydrophobic interface was quantified by means of the supermolecular approach at the MP2 level with solvation energy correction and compared with that of the hydrophilic interface of the BoNT/B – Syt-II complex. It was found that the energetic contribution of the hydrophobic interface toward binding of BoNT/B with Syt-II (-9.49 kcal/mol) is much larger than that of the hydrophilic interface (-2.58 kcal/mol). A pair-wise intermolecular interaction analysis was also performed to decipher the molecular determinants for recognition of BoNT/B by Syt-II. The interest lies in determining which types of interactions are used by the protein receptor Syt-II for recognition of BoNT/B, and what their relative importance is. It was discovered that π-π stacking interactions among aromatic residues act as the major molecular determinants for recognition of cell surface receptor Syt-II by the botulinum neurotoxin BoNT/B. Our findings are in good agreement with results of biophysical and site-directed mutagenesis experiments reported in the literature [31,32,55 ,57].

Acknowledgment

We are pleased to acknowledge the Ohio Supercomputer Center for a generous allocation of supercomputer time.

References

1. Schiavo G, Rossetto O, Montecucco C. Clostridial neurotoxins as tools to investigate the molecular events of neurotransmitter release. Seminars in Cell Biology. 1994; 5: 221-229.
2. Schiavo G, Matteoli M, Montecucco C. Neurotoxins affecting neuroexocytosis. Physiol Rev. 2000; 80: 717-766.
3. Simpson LL. The origin, structure, and pharmacological activity of botulinum toxin. Pharmacol Rev. 1981; 33: 155-188.
4. Arnon SS, Schechter R, Inglesby TV, Henderson DA, Bartlett JG, Ascher MSB, et al. Botulinum toxin as a biological weapon - Medical and public health management. JAMA-J. Am. Med. Assoc. 2001; 285: 1059-1070.
5. Hatheway CL. Botulism: the present status of the disease. Curr Top Microbiol Immunol. 1995; 195: 55-75.
6. Johnson EA. Clostridial toxins as therapeutic agents: benefits of nature's most toxic proteins. Annu Rev Microbiol. 1999; 53: 551-575.
7. Montecucco C, Papini E, Schiavo G. Bacterial protein toxins penetrate cells via a four-step mechanism. FEBS Lett. 1994; 346: 92-98.
8. Montecucco C, Schiavo G. Structure and function of tetanus and botulinum neurotoxins. Q Rev Biophys. 1995; 28: 423-472.
9. Andreas Rummel, irstin Häfner, Stefan Mahrhold, Natallia Darashchonak, Matthew Holt, Reinhard Jahn, et al. Botulinum neurotoxins C, E and F bind

gangliosides via a conserved binding site prior to stimulation-dependent uptake with botulinum neurotoxin F utilising the three is forms of SV2 as second receptor. Journal of Neurochemistry. 2009; 110: 1942-1954.

10. Rossetto O, Montecucco C. Peculiar binding of botulinum neurotoxins. ACS Chem Biol. 2007; 2: 96-98.

11. Willis B, Eubanks LM, Dickerson TJ, Janda KD. The Strange Case of the Botulinum Neurotoxin: Using Chemistry and Biology to Modulate the Most Deadly Poison. Angewandte Chemie-International Edition. 2008; 47; 8360-8379.

12. Montecucco C, Rossetto O, Schiavo G. Presynaptic receptor arrays for clostridial neurotoxins. Trends Microbiol. 2004; 12: 442-446.

13. Schiavo G, Osborne SL, Sgouros JG. Synaptotagmins: more isoforms than functions? Biochem Biophys Res Commun. 1998; 248: 1-8.

14. Südhof TC. Synaptotagmins: why so many? J Biol Chem. 2002; 277: 7629-7632.

15. Nishiki T, Kamata Y, Nemoto Y, Omori A, Ito T, Takahashi M. Identification of protein receptor for Clostridium botulinum type B neurotoxin in rat brain synaptosomes. J Biol Chem. 1994; 269: 10498-10503.

16. Tei-ichi Nishiki , Yoshimi Tokuyama , Yoichi Kamata , Yasuo Nemoto , Akira Yoshida, Kazuki Sato, et al. The high-affinity binding of Clostridium botulinum type B neurotoxin to synaptotagmin II associated with gangliosides G (T1b)/G (D1a). Febs Letters. 1996; 378: 253-257.

17. Rummel A, Karnath T, Henke T, Bigalke H, Binz T. Synaptotagmins I and II act as nerve cell receptors for botulinum neurotoxin G. J Biol Chem. 2004; 279: 30865-30870.

18. Min Dong, David A Richards, Michael C Goodnough, William H Tepp, Eric A Johnson , Edwin R Chapman. Synaptotagmins I and II mediate entry of botulinum neurotoxin B into cells. Journal of Cell Biology. 2003; 162, 1293-1303.

19. Feany MB, Lee S, Edwards RH, Buckley KM. The Synaptic Vesicle Protein Sv2 is a Novel Type of Transmembrane Transporter. Cell. 1992; 70: 861-867.

20. Bajjalieh SM, Peterson K, Shinghal R, Scheller RH. SV2, a brain synaptic vesicle protein homologous to bacterial transporters. Science. 1992; 257: 1271-1273.

21. Dong M, Yeh F, Tepp WH, Dean C, Johnson EA, Janz R. SV2 is the protein receptor for botulinum neurotoxin A. S Science. 2006; 312: 592-596.

22. Mahrhold S, Rummel A, Bigalke H, Davletov B, Binz T. The synaptic vesicle protein 2C mediates the uptake of botulinum neurotoxin A into phrenic nerves. FEBS Lett. 2006; 580: 2011-2014.

23. Dong M, Liu H, Tepp WH, Johnson EA, Janz R, Chapman ER. Glycosylated SV2A and SV2B mediate the entry of botulinum neurotoxin E into neurons. Mol Biol Cell. 2008; 19: 5226-5237.

24. Fu Z, Chen C, Barbieri JT, Kim JJ, Baldwin MR. Glycosylated SV2 and gangliosides as dual receptors for botulinum neurotoxin serotype F. Biochemistry. 2009; 48: 5631-5641.

25. Lacy DB, Tepp W, Cohen AC, DasGupta BR, Stevens RC. Crystal structure of botulinum neurotoxin type A and implications for toxicity. Nat Struct Biol. 1998; 5: 898-902.

26. Swaminathan S, Eswaramoorthy S. Structural analysis of the catalytic and binding sites of Clostridium botulinum neurotoxin B. Nat Struct Biol. 2000; 7: 693-699.

27. Kumaran D, Eswaramoorthy S, Furey W, Navaza J, Sax M, Swaminathan S. Domain organization in Clostridium botulinum neurotoxin type E is unique: its implication in faster translocation. J Mol Biol. 2009; 386: 233-245.

28. Brunger AT, Jin R, Breidenbach MA. Highly specific interactions between botulinum neurotoxins and synaptic vesicle proteins. Cellular and Molecular Life Sciences. 2008; 65: 2296-2306.

29. Lalli G, Herreros J, Osborne SL, Montecucco C, Rossetto O, Schiavo G. Functional characterization of tetanus and botulinum neurotoxins binding domains. J Cell Sci. 1999; 112: 2715-2724.

30. Halpern JL, Loftus A. Characterization of the receptor-binding domain of tetanus toxin. J Biol Chem. 1993; 268: 11188-11192.

31. Chai Q, Arndt JW, Dong M, Tepp WH, Johnson EA, Chapman ER, et al. Structural basis of cell surface receptor recognition by botulinum neurotoxin B. Nature. 2006; 444, 1096-1100.

32. Jin R, Rummel A, Binz T, Brunger AT. Botulinum neurotoxin B recognizes its protein receptor with high affinity and specificity. Nature. 2006; 444: 1092-1095.

33. Berntsson RP, Peng L, Dong M, Stenmark P. Structure of dual receptor binding to botulinum neurotoxin B. Nat Commun. 2013; 4: 2058.

34. DeLano WL. The PyMOL Molecular Graphics System. DeLano Scientific, San Carlos, CA, USA. 2002.

35. Johnson EA. Biomedical aspects of botulinum toxin. Journal of Toxicology-Toxin Reviews. 1999; 18; 1-15.

36. Lisong Mao, Yanli Wang , Yuemin Liu , Xiche Hu. Multiple intermolecular interaction modes of positively charged residues with adenine in ATP-binding proteins. Journal of the American Chemical Society. 2003; 125: 14216-14217.

37. Frisch MJ, Trucks GW, Schlegel HB, Scuseria GE, Robb MA, Cheeseman JR, et al. Revision C.02. Gaussian, Inc, Wallingford CT. 2004.

38. Boys SF, Bernardi F. The calculation of small molecular interactions by the differences of separate total energies. Some procedures with reduced errors. Mol. Phys. 1970; 19: 553-566.

39. Sponer J, Leszczynski J, Hobza P. Hydrogen bonding and stacking of DNA bases: a review of quantum-chemical ab initio studies. J Biomol Struct Dyn. 1996; 14: 117-135.

40. Del Bene JE, Shavitt I. The quest for reliability in calculated properties of hydrogen-bonded complexes. in Molecular Interactions, Wiley, Chichester. 1997; 157-180.

41. Hobza P, Zahradnik R. Intermolecular Interactions between Medium-Sized Systems- Nonempirical and Empirical Calculations of Interaction Energies – Successes and Failures. Chem. Rev. 1988; 88; 871-897.

42. Chalasinski G, Gutowski M. Weak-interactions between small systems - models for studying the nature of intermolecular forces and challenging problems for ab initio calculations. Chem. Rev. 1988; 88: 943-962.

43. AD Buckingham, PW Fowler, Jeremy M Hutson. Theoretical-Studies of van der Waals Molecules and Intermolecular Forces. Chem. Rev. 1988; 88; 963-988.

44. Tsuzuki S, Uchimaru T, Mikami M, Tanabe K. Basis set effects on the calculated bonding energies of neutral benzene dimers: Importance of diffuse polarization functions. Chemical Physics Letters. 1996; 252: 206-210.

45. Tsuzuki S, Uchimaru T, Tanabe K. Intermolecular interaction potentials of methane and ethylene dimers calculated with the Moller-Plesset, coupled cluster and density functional methods. Chemical Physics Letters. 1998; 287: 202-208.

46. Tarakeshwar P, Choi HS, Kim KS. Olefinic vs aromatic pi-H interaction: A theoretical investigation of the nature of interaction of first-row hydrides with ethane and benzene. J. Am. Chem. Soc. 2001; 123: 3323-3331.

47. Sponer J, Berger I, SpaÄ kovÃ¡ N, Leszczynski J, Hobza P. Aromatic Base Stacking in DNA: From ab initio Calculations to Molecular Dynamics Simulations. J Biomol Struct Dyn. 2000; 17 Suppl 1: 1-24.

48. Pavel Hobza, Jiri Sponer, Martin Polasek. H-Bonded and Stacked DNA-Base Pairs - Cytosine Dimer - an Ab- Initio 2nd-Order Moller-Plesset Study. J. Am. Chem. Soc.1995; 117: 792-798.

49. Li JB, Zhu TH, Hawkins GD, Winget P, Liotard DA, Cramer CJ, et al. Extension of the platform of applicability of the SM5.42R universal solvation model. Theor. Chem. Acc. 1999; 103: 9-63.

50. Xidos JD, Li J, Zhu T, Hawkins GD, Thompson JD, Chuang YY, et al. GAMESOL-version 3.1. 2002.

51. Michael W Schmidt, Kim K Baldridge, Jerry A Boatz, Steven T Elbert, Mark S Gordon, Jan H Jensen, et al. General atomic and molecular electronic-structure system. Journal of Computational Chemistry.1993; 14: 1347-1363.

52. Yanli Wang, Xiche Hu. A quantum chemistry study of binding carotenoids in the bacterial light-harvesting complexes. Journal of the American Chemical Society. 2002; 124: 8445-8451.

53. Mao L, Wang Y, Liu Y, Hu X. Molecular determinants for ATP-binding in proteins: a data mining and quantum chemical analysis. J Mol Biol. 2004; 336: 787-807.

54. Liu Y, Hu X. Molecular determinants for binding of ammonium ion in the ammonia transporter AmtB - A quantum chemical analysis. Journal of Physical Chemistry A. 2006; 110: 1375-1381.

55. Peng L, Berntsson RP, Tepp WH, Pitkin RM, Johnson EA, Stenmark P, et al. Botulinum neurotoxin D-C uses synaptotagmin I and II as receptors, and human synaptotagmin II is not an effective receptor for type B, D-C and G toxins. Journal of Cell Science. 2012; 125: 3233-3242.

56. Strotmeier J, Willjes G, Binz T, Rummel A. Human synaptotagmin-II is not a high affinity receptor for botulinum neurotoxin B and G: increased therapeutic dosage and immunogenicity. FEBS Lett. 2012; 586: 310-313.

57. Willjes G, Mahrhold S, Strotmeier J, Eichner T, Rummel A, Binz T. Botulinum Neurotoxin G Binds Synaptotagmin-II in a Mode Similar to That of Serotype B: Tyrosine 1186 and Lysine 1191 Cause Its Lower Affinity. Biochemistry. 2013; 52: 3930- 3938.

58. Stenmark P, Dong M, Dupuy J, Chapman ER, Stevens RC. Crystal structure of the botulinum neurotoxin type G binding domain: insight into cell surface binding. J Mol Biol. 2010; 397: 1287-1297.

59. Patocka J, Kuca K, Jun D. Botulinum toxin: Bioterror and biomedicinal agent. Defence Science Journal. 2006; 56: 189-197.